Study on the Rectification of Ionic Diode Based on Cross-Linked Nanocellulose Bipolar Membranes

Hongli Yang, Jesper Edberg, Mehmet Girayhan Say, Johan Erlandsson, Viktor Gueskine, Lars Wagberg, Magnus Berggren and Isak Engquist

Study on the Rectification of Ionic Diode Based on Cross-linked Nanocellulose Bipolar Membranes

Hongli Yang,[a,b,]* *Jesper Edberg,*[c] *Mehmet Girayhan Say,*[b] *Johan Erlandsson,*[d] *Viktor Gueskine,*[b,e] *Lars Wågberg,*[d,f] *Magnus Berggren,*[b,e] *Isak Engquist*[b,e]

[a]College of Polymer Science and Engineering, Sichuan University, Chengdu 610065, P. R. China.

[b]Laboratory of Organic Electronics, Department of Science and Technology, Linköping University, SE-601 74 Norrköping, Sweden

[c]RISE Research Institutes of Sweden, Digital Systems, Smart Hardware, Bio-, Organic and Printed Electronics, Norrköping 60233, Sweden.

[d]Division of Fibre Technology, Department of Fibre and Polymer Technology, School of Chemistry, Biotechnology and Health, KTH Royal Institute of Technology, SE-100 44 Stockholm, Sweden.

[e]Wallenberg Wood Science Centre, Department of Science and Technology, Linköping University, SE-601 74 Norrköping, Sweden.

[f]Wallenberg Wood Science Centre, Department of Fibre and Polymer Technology, School of Chemistry, Biotechnology and Health, KTH Royal Institute of Technology, SE-100 44 Stockholm, Sweden.

ABSTRACT

Nanocellulose-based membranes have attracted intense attention in bioelectronic devices due to their low cost, flexibility, biocompatibility, degradability, and sustainability. Herein, we demonstrate a flexible ionic diode using a cross-linked bipolar membrane fabricated from positively and negatively charged cellulose nanofibrils (CNFs). The rectified current originates from the asymmetric charge distribution which can selectively determine the direction of ion transport inside the bipolar membrane. The mechanism of rectification was demonstrated by electrochemical impedance spectroscopy with voltage biases. The rectifying behavior of this kind of ionic diode was studied by using linear sweep voltammetry to obtain current-voltage characteristics and time dependence of the current. In addition, the performance of cross-linked CNF diodes was investigated while changing parameters such as the thickness of the bipolar membranes, scanning voltage range, and scanning rate. A good long-term stability due to the high density cross-linking of the diode was shown in both current-voltage characteristics and time dependence of current.

INTRODUCTION

The junction between p-type and n-type semiconductors is a critical part of many electronic devices due to the asymmetric charge transport at the interface which only enables the transport of electrons/holes in one direction, known as rectification.[1,2] These electronics are the building blocks of modern digital technology due to their unique junction structure, such as diodes, photovoltaic cells, transistors.[3-8] In biology, it is ions in liquids rather than electrons in solids which are the charge carrying particles used for different functions. For this reason, ions as signal carriers play essential roles in bioelectronic devices for applications such as ionic circuitry,[9] sensory systems,[10] and smart gating.[11,12]

The formation of a rectified junction by using two oppositely charged nanochannels,[13–15] membranes,[16,17] or polyelectrolyte gels[18,19] has been demonstrated in an ionic diode, which was responsible for unidirectional ionic current across the junction interface. The junction with charged nanochannels and microfluidic chips enables to efficiently rectify the ionic current due to their unique nanostructure.[14,20] However, the complicated fabrication process, i.e, microfabrication, and the fluid in the channel impose challenges in the device encapsulation for practical applications. In addition, with the development of wearable electronics, there is an additional demand of flexibility for certain electronic or ionic devices.[21-23] Recently, ion-selective membranes and polyelectrolyte gels which usually made from nondegradable polymers have been developed for use in flexible devices, including diodes,[18,24] and transistors.[18,25] To avoid electronic waste and move towards sustainable devices, biodegradable and renewable materials are urgently needed to manufacture these devices.[26]

Cellulose materials have attracted particular interest due to its abundant resources, sustainability and biodegradability. Recently, researchers have studied ionic diode based on cellulose materials, including asymmetrically charged micro-fibrillated cellulose-based paper and cellulose nanocrystal-agarose hydrogel for ionic diodes.[27,28] However, the detailed principles and long-term rectification of those cellulose-based ionic diodes remain unclear. Cellulose nanofibrils (CNFs), which can be extracted from wood and possess excellent mechanical properties and shape flexibility due to the high aspect ratio,[29,30] have been one of potential candidates for flexible iontronics (electronic devices using ions as charge carriers). In addition, CNF has great potential for the desired functionality due to the abundance of hydroxyl groups, available for functionalization, on the cellulose chain. It provides a great chance to fabricate CNF-based bipolar membranes with oppositely charged layers through different modifications.[31-33] However, CNF-based membranes have poor wet-stability since water molecules will decrease the attraction between the fibrils due to the high polarity of the cellulose as well as a high dispersive surface energy of cellulose, which limits their application in water-tolerant devices. Covalent cross-linking is a reliable solution to address the above issue by using nontoxic crosslinkers, such as poly (carboxylic acids), and epoxy-functionalized polyethylene glycols.[34-36]

In this work, we combined cross-linked anionic and cationic CNF membranes to fabricate ionic diodes. The negatively- and positively charged CNF layers were cross-linked by 1,2,3,4-butanetetracarboxylic acid (BTCA) and poly (ethylene glycol) diglycidyl ether (PEGDE), respectively, to obtain bipolar membranes with excellent mechanical performance and water stability. The rectification mechanism of the ionic diode can be understood through different diffusion/migration behaviors of mobile ions under forward and reverse biases in the cross-linked CNF bipolar membranes. The detailed rectification process was investigated through linear sweep voltammetry and time dependence of current under constant voltage (chronoamperometry), which results indicate that the ionic bipolar membrane exhibits long-term rectification. These bipolar membranes have potential in the application of low-cost, flexible, biocompatible electronic devices.

METHODS

Materials: Carboxymethylated cellulose nanofibrils (CNF) were provided by RISE Bioeconomy and Health, Sweden. Never dried dissolving pulp was supplied by Domsjö Fabriker (Örnsköldsvik, Sweden). All chemicals, 1, 2, 3, 4-butane tetracarboxylic acid (BTCA), sodium hypophosphite (SHP), glycerol, poly (ethylene glycol) diglycidyl ether (PEGDE, Mn 500), sodium hydroxide (NaOH), hydrochloric acid (HCl), and glycidyltrimethylammonium chloride were purchased from Sigma-Aldrich and used as received. Indium tin oxide (ITO) coated polyethylene terephthalate (PET) with the surface resistivity of 10 Ω/sq was purchased from Sigma-Aldrich. Experiments were carried out with deionized water.

Preparation of cationic CNFs: The wood-derived cationic CNFs were prepared using a procedure similar to that described earlier.[37] Never dried fibres were added to a mixture of 2-propanol and water to form a 65 g/L fibre suspension with a final 2-propanol: water ratio of 40:60 (v/v). Note that the amount of water associated with the never dried fibres have been considered. 13 g of NaOH was subsequently dissolved in the fibre suspension before adding glycidyltrimethylammonium chloride corresponding to 4 g/g of dry fibre to the mixture. The fibre dispersion was subsequently mixed thoroughly and allowed to incubate for 30 minutes at room temperature before the reaction was initiated by heating the mixture to 60°C for 6h. The modified fibres were then washed with excessive amounts of water in a Büchner funnel to remove solvents and reagents followed by soaking in a 0.1M HCl solution for 30 minutes and another washing step. CNFs were subsequently prepared from the chemically modified fibres by high-pressure homogenization using a M-110 EH

Microfluidizer (Microfluidics Corporation, Westwood, MA) by firstly passing the fibres through 400μm/200μm sequentially assembled chambers at 800 bar one time and secondly through 200μm/100μm chambers one time at 1500 bar. The collected CNFs were stored refrigerated at 4°C until further use.

Preparation of bipolar membranes: Firstly, the anionic CNF membrane with negative charges which is the 20 wt% BTCA cross-linked carboxymethylated CNF membrane was fabricated by using the same method as previous work.[35] 20 wt% PEGDE was added to the cationic CNF suspension with solid content of 0.3 %, and the mixture was mixed using a lab homogenizer (T-10 ULTRA TURRAX, IKA). The following cross-linking reaction was performed at 70 °C for 3 h. After degassing, the mixture was poured on top of the dry anionic membrane. The bipolar membrane can be obtained after overnight drying at 60 °C. The thickness ratio between cationic and anionic membranes of the bipolar membrane was controlled by tuning the volume of cationic and anionic suspensions.

Characterization: The charge density of the cationic CNFs was determined by colloidal titration of dispersed CNFs using a Stabino potential analyzer (Microtrac Retsch GmBH, Germany) and using potassium poly (vinyl sulfate) as titrant. The Fourier transform infrared (FTIR) spectra of the membrane were measured in the attenuated total reflectance (ATR) mode by using an Equinox 55 (Bruker) instrument. The spectra were recorded in the wavenumber range from 4000 to 400 cm^{-1} and with a resolution of 4 cm^{-1}. The cross-sectional images of the bipolar membrane were collected by scanning electron microscopy (Zeiss). The energy-dispersive X-ray spectroscopy (EDS) mapping images were collected and processed using the same instrument equipped with the Oxford Aztec EDS system.

Diode measurements: The bipolar membrane (2 cm × 2 cm) was wetted with deionized water and then laminated between the two ITO electrodes. Electrochemical impedance spectroscopy (EIS) under DC voltage biases were measured over a frequency range of 100 kHz to 100 mHz and an AC voltage amplitude of 10 mV. The characteristic current-voltage (I – V) curves were measured by sweeping bias voltage under different scan rates. EIS, I – V curves and chronoamperometry were all measured using a BioLogic SP200 potentiostat.

RESULTS AND DISCUSSION

Preparation and characterization of cross-linked CNF bipolar membranes

The pristine (non-crosslinked) anionic (p-type) and cationic (n-type) cellulose nanofibrils were prepared through chemical modification to introduce carboxymethyl ($-CH_2COOH$ or $-CH_2COONa$) and quaternary amine ($-[N(CH_3)_3]^+Cl^-$) groups, separately. The membranes were prepared by further cross-linking of modified CNFs to improve their water stability (the water stability of the PEGDE cross-linked cationic membrane is shown in Figure S1 in Supporting Information). The cross-linking of anionic CNF (ACNF) works through the esterification between carboxyl groups of the crosslinker BTCA and hydroxyl groups on the CNF (Figure 1a) while cationic CNF (CCNF) was cross-linked by the reactivity of epoxy groups on the crosslinker PEGDE toward hydroxyl groups on the CNF (Figure 1b). Furthermore, the cross-linking process using BTCA as a crosslinker provides additional negative charges on the surface of ACNF due to the unreacted carboxyl acid groups of BTCA. The previous conductometric titration results show that the cross-linked ACNF has a final charge density of 2735 μeq/g compared with the original ACNF with a charge density of 637 μeq/g,[35] whereas the charge density of CCNF is 650 μeq/g determined by colloidal titration.

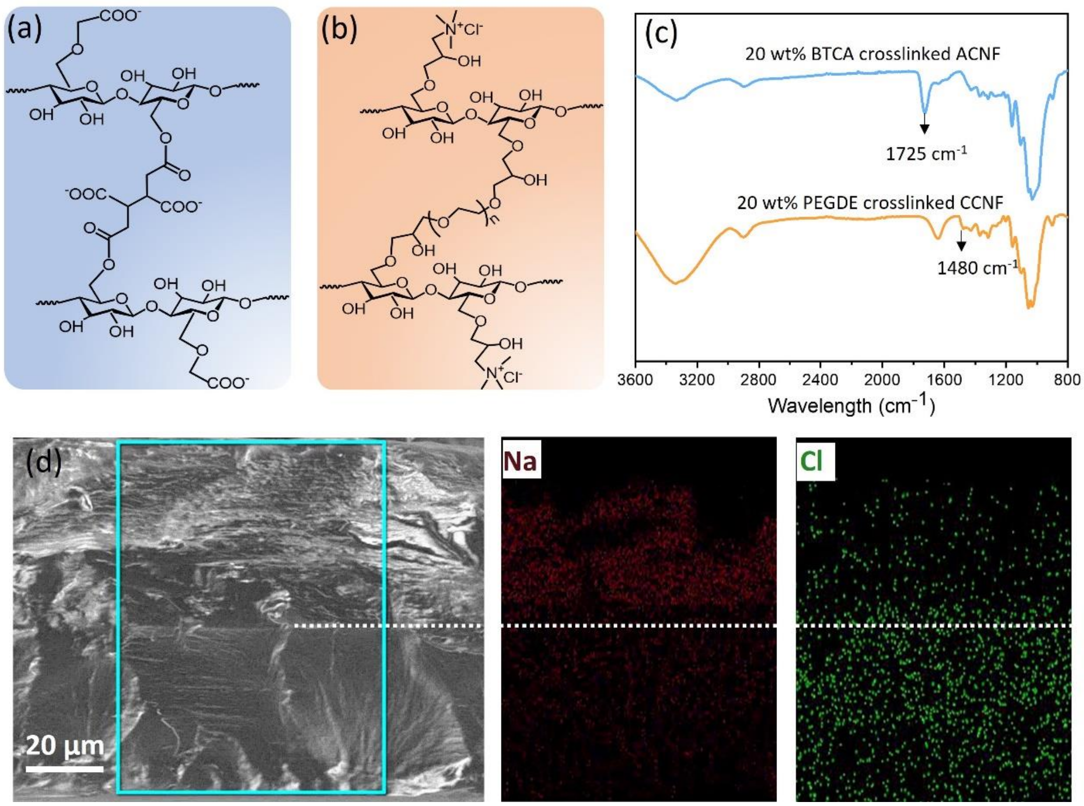

Figure 1. Structure of cross-linked CNF bipolar membrane. (a) the chemical structure of BTCA cross-linked anionic CNF; (b) the chemical structure of PEGDE cross-linked cationic CNF; (c) ATR-FTIR spectrum of two surfaces of bipolar membrane; (d) SEM image and EDS mapping of the cross-sectional bipolar membrane (the top membrane is made from anionic CNF and the bottom from cationic CNF).

To produce the bipolar membranes, the cross-linked ACNF membrane was first fabricated, after which the CCNF suspension, together with the crosslinker, was poured on top of the ACNF membrane. After drying, a bipolar membrane with two oppositely charged layers was obtained. ATR-FTIR spectra were measured for the two CNF membrane layers and is shown in Fig 1c. For the ACNF layer, the peak at 1725 cm^{-1} corresponds to the stretching of the C=O group, which relates to ester groups and carboxyl groups. There is a typical peak at 1480 cm^{-1}, corresponding to the trimethyl groups of the quaternary ammonium in the ACNF layer.[37] A cross-sectional SEM image and EDS element mapping of the membrane are displayed in Fig 1d. There is a clear interface but no gap between the positive and negative CNF layers, indicating a strong adhesion between the two sublayers. EDS mapping indeed shows the asymmetrical distribution of sodium and chloride ions in the two layers.

Mechanism of ionic diodes

The rectification behavior of the diode originates from the difference in concentration of mobile ions in the bipolar membrane junction under different voltage bias polarity. The ionic diode was operated by placing a piece of wet cross-linked CNF bipolar membrane between two ITO electrodes. When a bias voltage is applied, dissociation of water is expected at voltages above 1.23 V. The mobile counterions (Na^+, Cl^-), as well as protons and hydroxide ions generated by water dissociation, will migrate in the electric field to conduct current. The schematic of the working mechanism of the ionic diode is shown in Figure 2. Under a forward bias, the anode was in contact with the ACNF layer while the cathode was in contact with the CCNF layer. Protons generated at the anode and sodium counterions can pass through the ACNF layer, and hydroxide generated at the cathode and chloride counterions can move through the CCNF layer. Protons and hydroxide ions combine together to form water at the ACNF/CCNF interface, completing the circuit. Meanwhile, sodium and chloride ions can also migrate inside the layers and accumulate in the junction. Above process provides high conductivity of the bulk of bipolar membrane. In contrast, under a reverse bias, counter-ions move from the junction towards opposite sides of bipolar membrane, resulting in a depletion region and a large potential drop around the junction.[38] The potential drop enhances the water dissociation to generate protons and hydroxide ions which then move away from junction. In this depletion region, there is the formation of an ionic double layer (IDL) from immobile charges at the ACNF/CCNF interface and high resistance of junction.[24] The lower concentration of ions and high resistance at the junction lead to limited electric currents in reverse applied voltages.

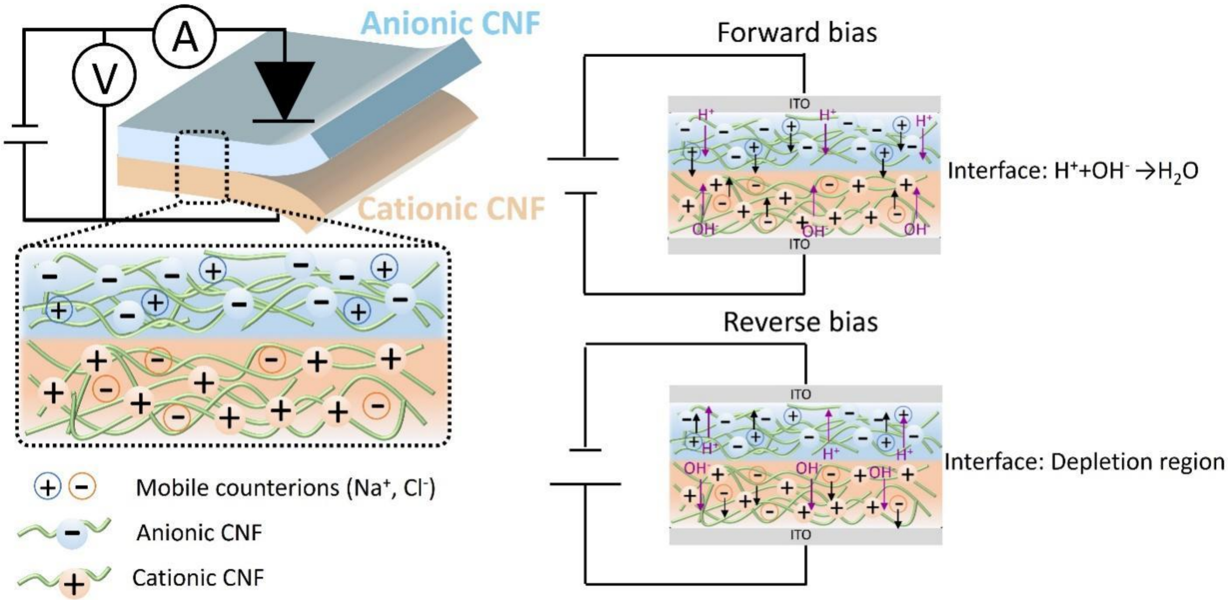

Figure 2. Schematic description of rectification mechanism of ionic diode based on cross-linked CNF bipolar membranes. The forward bias refers that the anode is in contact with the ACNF layer.

The rectification mechanism of the CNF bipolar membrane was studied by measuring EIS under different DC biases, with the corresponding Nyquist plot and Bode plot shown in Figure 3a and 3b. The fitted Nyquist plot under 0 V and the equivalent circuit model are shown in Figure S2 in Supporting Information. When the forward biases increased, the decrease in impedance of Nyquist plot in the low-frequency region can be attributed to decreasing resistance due to fast migration of ions towards the junction interface. Meanwhile, the phase angle of Bode phase plot corresponding to the IDL capacitance decreased in the low-frequency region, resulting from the destroyed IDL due to the accumulation of mobile counterions at the interface. The above phenomenon is intensified for biases up to +3 V, which is the consequence of more protons and hydroxides generated under high applied bias. Conversely, under a reverse bias, the slightly increased impedance and phase angle in the low-frequency region derive from the formation of a depletion region at the interface between the two membrane layers.

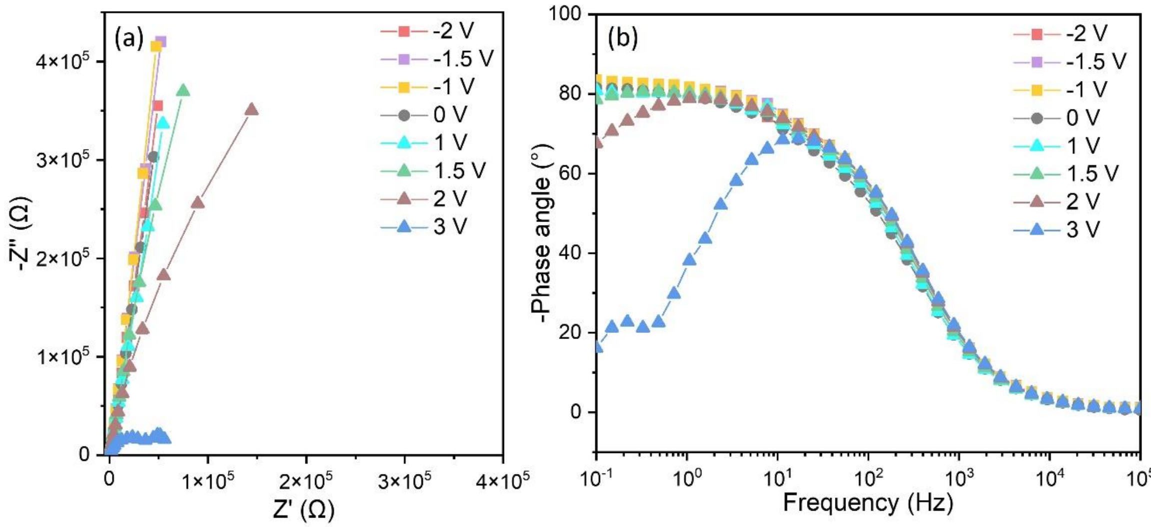

Figure 3. (a) Nyquist plot and (b) Bode phase plot of 50 μm ACNF / 55 μm CCNF bipolar membrane under dc biases.

Rectification behavior in voltage sweep

The rectification of the ionic diode was investigated by linear sweep voltammetry to measure current-voltage ($I - V$) characteristics. Before each measurement, the bipolar membrane was soaked in deionized water for the redistribution of ions back to their original equilibrium state. The $I - V$ curves of the bipolar membrane (with a thickness of 50 μm ACNF + 55 μm CCNF) were swept in different directions under different applied voltage ranges are shown in Figure 4. All curves were swept with a rate of 5 mV/s. At the beginning of sweeping, a current that drops fast can be monitored for both positive and negative applied bias, which results from the transient response of ions due to the suddenly applied voltage. This behavior can also be found in the CCNF or ACNF monolayer membranes (Figure S3). When the negative bias is applied, only counterions migrate to generate the transient current in the membranes. In contrast, proton, hydroxide, and counterions pass through the membrane under the positive bias. As a result, the initial currents at a negative bias (-2 V, -3 V, and -5 V) are lower than the values at a positive bias (+2 V, +3 V, and +5 V). When the voltage is scanned back (red curves in Figure 4), there is no transient response which is seen as a significant difference in the recorded current between the beginning of the black curves and the end of the red curves. Therefore, it is not reliable to evaluate the rectification ratio by using the ratio of the maximum current at the forward bias to the maximum current at the reverse bias in the first sweeping half-cycle since it would be an unfair evaluation where one current is transient while another current is steady. To describe reliably the rectification ratios, we only calculate their values using the curves after the first sweeping half-cycle in the current-voltage characteristics, and the rectification ratio is calculated by the ratio of maximum current under positive and negative voltages.

The electrolysis of water molecules occurs when the applied voltage bias is over the oxidation-reduction potential of water (1.23 V at 25 °C) which leads to the production of proton and hydroxide ions. However, during the sweep range between -2 V and +2 V, the current is quite low and there is no obvious rectification in the red curves which is due to very limited proton and hydroxide ions at +2 V. With the increase of the bias, more proton, and hydroxide ions were generated, resulting in a higher current and rectification ratio (the ratio increased from 3.5 at +3 V/-3 V to 6.2 at +5 V/-5 V in the red curves). The rectification ratio shows a lower value in this cross-linked CNF bipolar membrane compared to other related work,[27,28] the possible reason is the limitation of ion selectivity from cationic CNF membranes due to their low charge density (637 μeq/g) and intensive swelling in the wet state. In addition, the rectification ratio of the red curve in Figure 4b (3.5) is higher than the one in Figure 4e (1.5), and the same phenomenon occurs for the sweep bias range of -5 V − +5 V (Figure 4c and 4f). This suggests that the sweep direction also has a significant influence on the rectifying behavior of the diode. If the sweep started from the positive bias voltage (the black arrows in Figure 4e, 4f), as the above mechanism part discussed, proton and hydroxide ions generated at the electrode-membrane interfaces can pass through the membrane sublayers and meet at the junction to form water, resulting in the loss of water at the electrodes. When the sweep went from the negative bias voltage back to the positive bias voltage (the red arrows in Figure 4e, 4f), less water dissociated compared to the initial sweep point which led to the decreased current and rectification ratio.

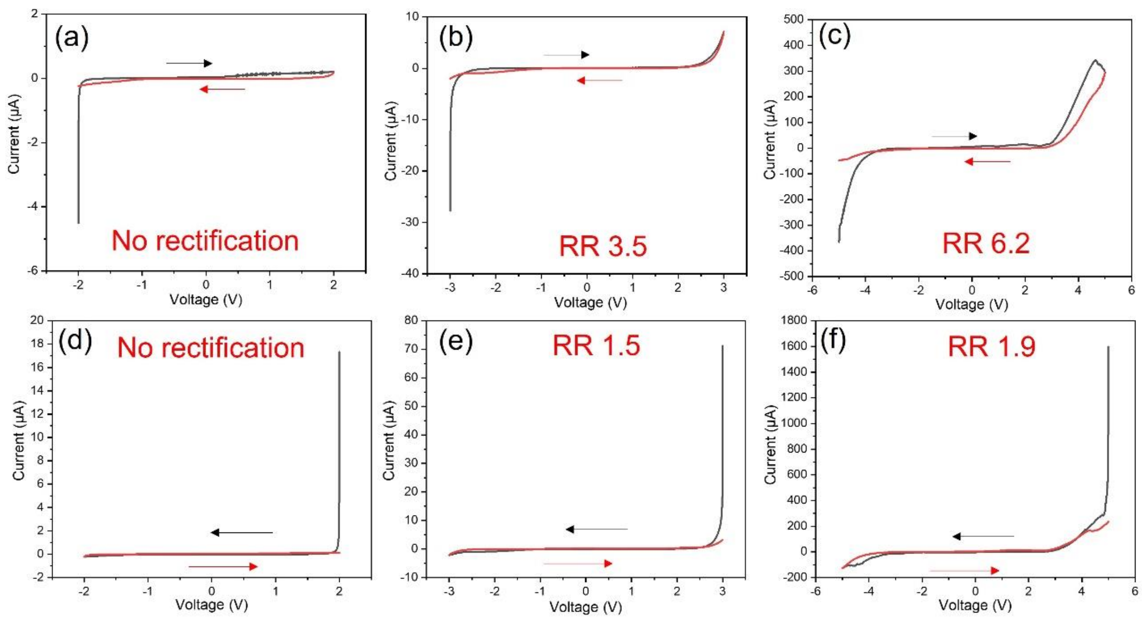

Figure 4. Current as a function of applied bias plots for 50 μm ACNF + 55 μm CCNF bipolar membrane with the scan rate of 5 mV/s and the sweeping direction of (a) -2 V→+2 V→-2 V; (b) -3 V→+3 V→-3 V; (c) -5 V→+5 V→-5 V; (d) +2 V→-2 V→+2 V; (e) +3 V→-3 V→+3 V; (f) +5 V→-5 V→+5 V. (RR denotes rectification ratio).

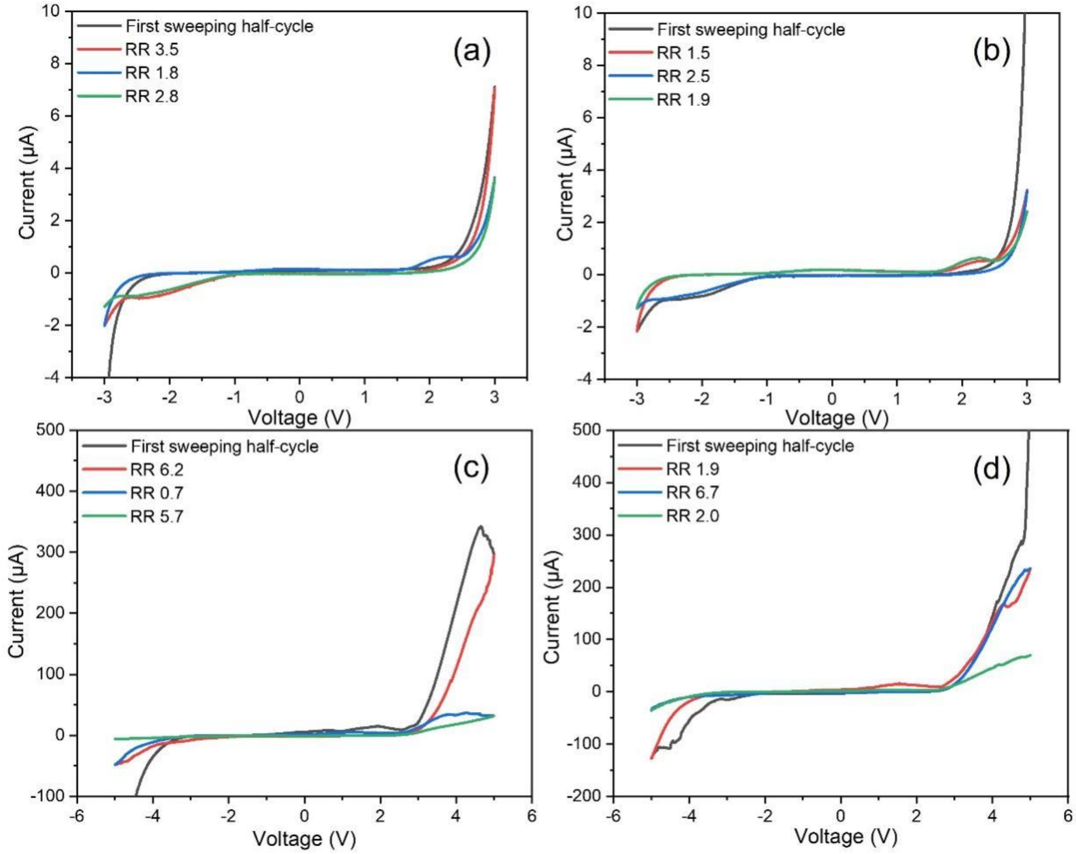

Figure 5. Current as a function of applied bias plots with two sweeping cycles for 50 μm ACNF + 55 μm CCNF bipolar membrane with the scan rate of 5 mV/s under the voltage range of (a) and (b) -3 V − +3 V; (c) and (d) -5 V − +5 V. (RR represents rectification ratio)

The long-term rectification of the ionic diode was further investigated through sweeping for several cycles. Figure 5 shows the current decays for consecutive sweeping in both forward and reverse bias due to consumption and evaporation of water during the measurement. The black, red, blue and green curves represent the first, second, third and fourth sweeping half-cycles, respectively. It is worth noting that the current drops significantly for -5 V – +5 V compared to -3 V – +3 V which is possibly attributed to the degradation of ITO under higher voltage.[39] Furthermore, there are always higher rectification ratios in the sweep direction from positive to negative bias compared to the values from negative bias to positive bias wherever the starting point of the sweep is. This can be understood from the perspective of water loss at the interface between the membrane and the ITO electrode under the forward bias as already discussed above. In addition, there is not a significant reduction in rectification ratio with the cycling if we only consider the value swept in the same direction. The same conclusion can be made from Figure S4, which shows 5 sweeping cycles of 50 μm ACNF + 55 μm CCNF bipolar membrane. The decreased current with cycling should be owing to the water loss. These results indicate that there is a potential for continued rectification behavior for several cycles, as long as the bipolar membrane is prevented from drying. Thus, this cross-linked CNF bipolar membrane might have limitations in real applications where water is not able to be sustained.

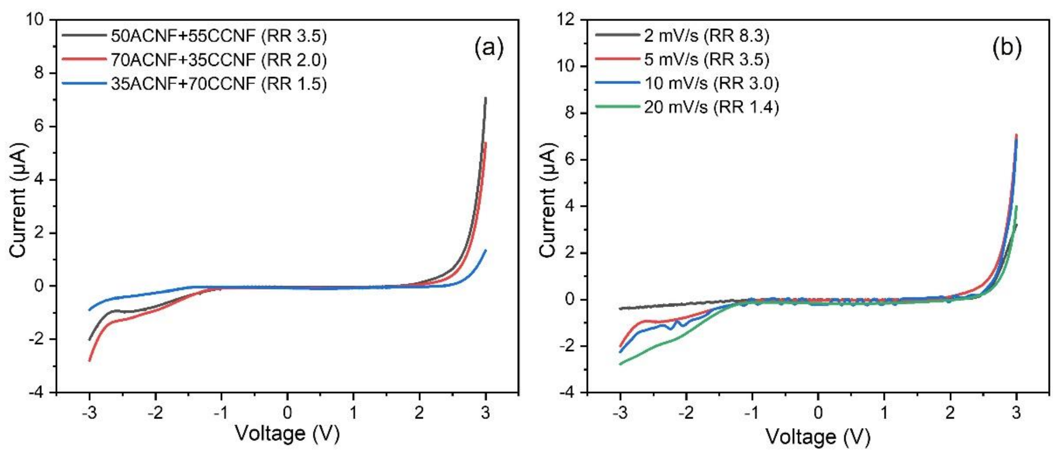

Figure 6. (a) Current as a function of applied bias plots for bipolar membranes with different thickness ratios under the scan rate of 5 mV/s; (b) Current as a function of applied bias plots for 50 μm ACNF + 55 μm CCNF bipolar membrane with different scan rates. (RR represents rectification ratio)

We also investigated the effect of the thickness ratio and the scan rate on the functions of the diode. To compare equally and parallelly, all curves in Figure 6 were selected from curves that were swept in the same direction as the red curve in Figure 4b, which means the back sweep from

+3 V to -3 V after the first sweep from -3 V to +3 V. The rectification ratio was calculated by the ratio of the current at +3V to the current at -3 V. Figure 6a shows that the bipolar membrane with thickness ratio of around 1:1 (50 μm ACNF + 55 μm CCNF) exhibits the optimal rectification ratio compared to the thickness ratios of 2:1 (70 μm ACNF + 35 μm CCNF) and 1:2 (35 μm ACNF + 70 μm CCNF). This could have two causes: one is that when the ions need to go through a longer distance, this results in increased resistance when a forward bias is applied; another is that it is easier for the ions to pass through a thinner layer which leads to higher conductivity under a reverse bias.[9, 11] Therefore, if the total thickness of the bipolar membrane is fixed, when the thickness of the two sublayers is similar, the diode shows a higher rectification ratio. The influence of scan rate on the rectification ratio of the bipolar membrane with 50 μm ACNF + 55 μm CCNF is illustrated in Figure 6b. The result shows the lower the scan rate, the higher the rectification ratio. This is possibly due to enough response time for the ions to equilibrate under the applied voltage and come to a steady state under a low sweep scan rate.

Time dependence of current in the ionic diode

The current response of the cross-linked CNF diode with 50 μm ACNF + 55 μm CCNF to an alternating electric field was recorded (Figure 7a-7c, Figure S5a-S5c in Supporting Information). As shown in Figure 7a - 7c, the current in the forward bias is always higher than that in the reverse bias during the cycles when the applied voltage is over 2 V which indicates that the cross-linked CNF-based diode exhibits good current rectification. In addition, the rectification becomes better with the increase of input voltage. These results are consistent with the conclusion from Figure 4. Furthermore, a large transient current is noticed after switching between forward and reverse bias. This is possibly due to fast rearrangement of ionic charges within the component, as discussed in connection with Figure 4. It is noted that the current reaches a steady state in a short time (within 20 seconds) whereafter the rectification behavior is restored.

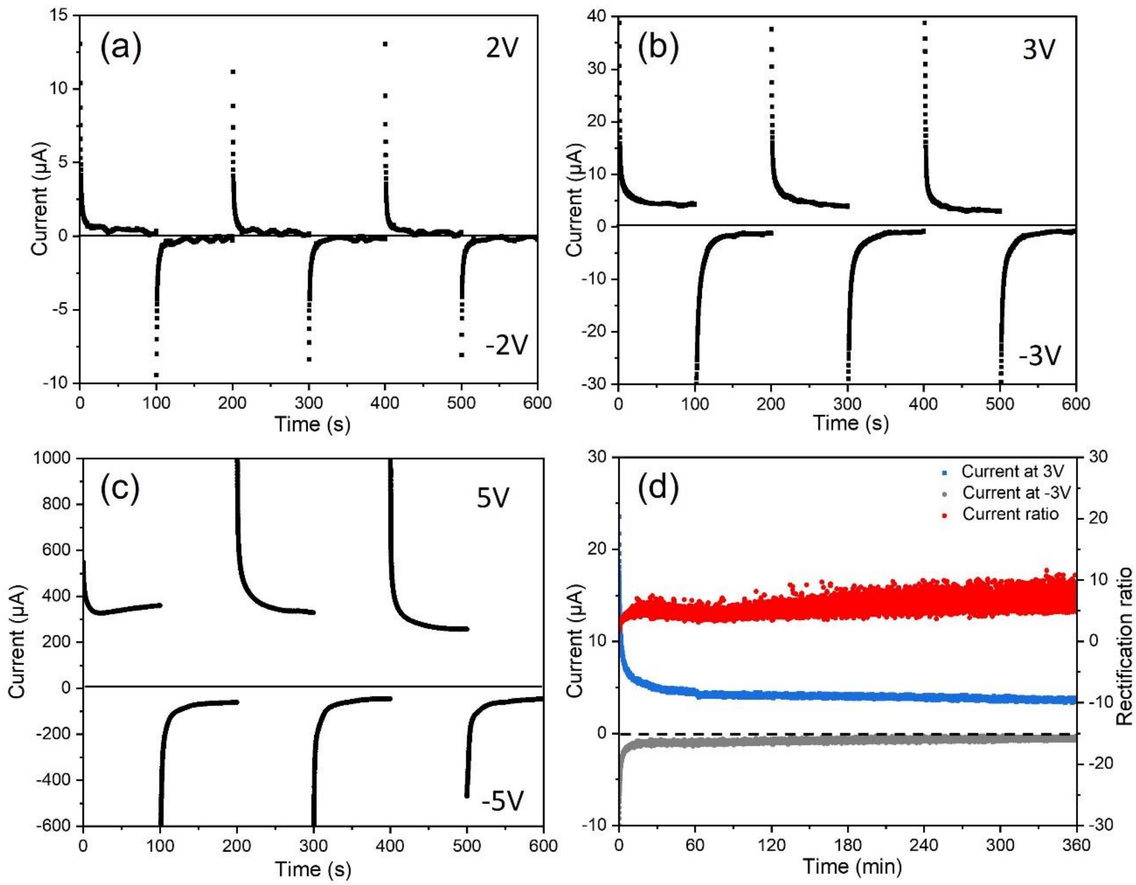

Figure 7. The current response of ionic diode at applied potentials of (a) ±2 V; (b) ±3 V; (c) ±5 V. Time dependence plot of current and corresponding rectification ratio under the constant forward (+3 V) and reverse (-3 V) bias.

The long-term rectification stability of the cross-linked CNF diode was demonstrated by monitoring the current response at constant positive (+3 V) and negative (-3 V) bias for six hours at each voltage, using a 50 μm ACNF + 55 μm CCNF membrane. The rectification ratio was calculated from the current ratio for a bias of ±3 V, and results are shown in Figure 7d. After the measurement under +3 V, the bipolar membrane was soaked in water for the redistribution of counterions for 2 h, and then the measurement under -3 V continued. For both biases, the current decreases rapidly from the initial value due to the transient response of ions at the beginning and gradually tends to a stationary one. The slight decay of the current in the steady-state can be attributed to water loss during the test. Even though the current drops, the rectification ratio increases from around 3 during the first two minutes to a stable range of around 5-10 when the current reaches a steady state. These data show that the cross-linked CNF diode exhibits a good capacity for continuous operation during several hours, and a long-term stable rectifying behavior.

CONCLUSIONS

In summary, we have demonstrated the rectifying behavior of an ionic diode fabricated from two layers of oppositely charged, cross-linked CNF membranes. The freestanding, wet-stable and flexible CNF bipolar membranes show good water stability due to the covalent cross-linking. The rectification of the ionic diode is achieved through selective transport of counterions under electric fields and the formation of an ionic double layer at the junction interface. The results from continuous linear sweeps and time-dependent current measurements indicate good long-term rectification. Therefore, the cross-linked nanocellulose-based bipolar membrane has a promising potential for usage in ionic logic gates, energy harvesting, and bioelectronics.

ASSOCIATED CONTENT

Supporting information

Pictures of non-crosslinked and PEGDE crosslinked cationic CNF membranes, Nyquist plot of AC-impedance measurement and equivalent circuit model, *C*-*V* curves of CNF monolayer membranes, long stability test with 5 sweeping cycles, applied voltage with time plot

ACKNOWLEDGMENTS

We acknowledge VINNOVA (Digital Cellulose Centre), Knut and Alice Wallenberg Foundation (Wallenberg Wood Science Center) for financial support. We also acknowledge RISE Bioeconomy and Health for the supply of carboxymethylated CNF.

REFERENCES

(1) Leger, J. M.; Rodovsky, D. B.; Bartholomew, G. P. Self-Assembled, Chemically Fixed Homojunctions in Semiconducting Polymers. *Adv. Mater.* **2006**, *18*, 3130-3134.

(2) Cheng, C. H. W.; Lonergan, M. C. A Conjugated Polymer pn Junction. *J. Am. Chem. Soc.* **2004**, *126*, 10536–10537.

(3) Trahms, M.; Melischek, L.; Steiner, J. F.; Mahendru, B.; Tamir, I.; Bogdanoff, N.; Peters, O.; Reecht, G.; Winkelmann, C. B.; Von Oppen, F.; Franke, K. J. Diode Effect in Josephson Junctions with a Single Magnetic Atom. *Nature* **2023**, *615*, 628–633.

(4) Wang, J.; Wang, Y.; Li, K.; Dai, X.; Zhang, L.; Wang, H. Lateral Fully Organic P–N Diodes Created in a Single Donor–Acceptor Copolymer. *Adv. Mater.* **2022**, *34*, 2106624.

(5) Liu, J.; Engquist, I.; Berggren, M. Double-gate light-emitting electrochemical transistor: confining the organic p–n junction. *J. Am. Chem. Soc.* **2013**, *135*, 12224-12227.

(6) Aftab, S.; Zahir Iqbal, M.; Hussain, S.; Hegazy, H. H.; Kabir, F.; Hassan Abbas Jaffery, S.; Koyyada, G. New Developments in Gas Sensing Using Various Two-Dimensional Architectural Designs. *Chemical Engineering Journal* **2023**, *469*, 144039.

(7) Wang, C.; Fu, B.; Zhang, X.; Li, R.; Dong, H.; Hu, W. Solution-processed, large-area, two-dimensional crystals of organic semiconductors for field-effect transistors and phototransistors. *ACS Cent. Sci.* **2020**, *6*, 636-652.

(8) Nayak, P. K.; Mahesh, S.; Snaith, H. J.; Cahen, D. Photovoltaic solar cell technologies: analysing the state of the art. *Nat. Rev. Mater.* **2019**, *4*, 269-285.

(9) Janson, P.; Gabrielsson, E. O.; Lee, K. J.; Berggren, M.; Simon, D. T. An ionic capacitor for integrated iontronic circuits. *Adv. Mater. Technol.* **2019**, *4*, 1800494.

(10) Du, M.; Zhang, D.; Fan, W.; Zhao, K.; Xia, Y.; Nie, Z.; Sui, K. Ionic Diode-Based Self-Powered Ionic Skins with Multiple Sensory Capabilities. *Mater. Today Phys.* **2022**, *26*, 100744.

(11) Sabbagh, B.; Fraiman, N. E.; Fish, A.; Yossifon, G. Designing with Iontronic Logic Gates─From a Single Polyelectrolyte Diode to an Integrated Ionic Circuit. *ACS Appl. Mater. Interfaces* **2023**, *15*, 23361–23370.

(12) Grey, P.; Fernandes, S. N.; Gaspar, D.; Deuermeier, J.; Martins, R.; Fortunato, E.; Godinho, M. H.; Pereira, L. Ionically Modified Cellulose Nanocrystal Self-Assembled Films with a Mesoporous Twisted Superstructure: Polarizability and Application in Ion-Gated Transistors. *ACS Appl. Electron. Mater*. **2020**, *2*, 426–436.

(13) Li, J.; Li, D. Integrated Iontronic Circuits Based on Single Nanochannels. *ACS Appl. Mater. Interfaces* **2021**, *13*, 48208–48218.

(14) Kim, J.; Jeon, J.; Wang, C.; Chang, G. T.; Park, J. Asymmetric Nanochannel Network-Based Bipolar Ionic Diode for Enhanced Heavy Metal Ion Detection. *ACS Nano* **2022**, *16* , 8253–8263.

(15) Wang, Y.; Zhai, J. Cell Junction Proteins-Mimetic Artificial Nanochannel System: Basic Logic Gates Implemented by Nanofluidic Diodes. *Langmuir* **2019**, *35*, 3171–3175.

(16) Li, J.; Zhang, K.; Li, D. pH-Regulated Ionic Diode Based on an Asymmetric Shaped Multiple-Layer Polymer Membrane. *Anal. Chem.* **2023**, *95*, 1419–1427.

(17) Bao, B.; Hao, J.; Bian, X.; Zhu, X.; Xiao, K.; Liao, J.; Zhou, J.; Zhou, Y.; Jiang, L. 3D Porous Hydrogel/Conducting Polymer Heterogeneous Membranes with Electro-/PH-Modulated Ionic Rectification. *Adv. Mater.* **2017**, *29*, 1702926.

(18) Kim, H. J.; Chen, B.; Suo, Z.; Hayward, R. C. Ionoelastomer Junctions between Polymer Networks of Fixed Anions and Cations. *Science* **2020**, *367*, 773–776.

(19) Zhang, Y.; Jeong, C. K.; Wang, J.; Chen, X.; Choi, K. H.; Chen, L.-Q.; Chen, W.; Zhang, Q. M.; Wang, Q. Hydrogel Ionic Diodes toward Harvesting Ultralow-Frequency Mechanical Energy. *Adv. Mater.* **2021**, *33*, 2103056.

(20) Peng, R.; Pan, Y.; Liu, B.; Li, Z.; Pan, P.; Zhang, S.; Qin, Z.; Wheeler, A. R.; Tang, X. (Shirley); Liu, X. Understanding Carbon Nanotube-Based Ionic Diodes: Design and Mechanism. *Small* **2021**, *17*, 2100383.

(21) Xie, W.; Duan, J.; Wang, H.; Li, J.; Liu, R.; Yu, B.; Liu, S.; Zhou, J. Ultra-Stretchable, Bio-Inspired Ionic Skins That Work Stably in Various Harsh Environments. *J. Mater. Chem. A* **2018**, *6*, 24114–24119.

(22) Cao, Y.; Morrissey, T. G.; Acome, E.; Allec, S. I.; Wong, B. M.; Keplinger, C.; Wang, C. A transparent, self-healing, highly stretchable ionic conductor. *Adv. Mater.* **2017**, *29*, 1605099.

(23) Aftab, S.; Hussain, S.; Al-Kahtani, A. A. Latest Innovations in 2D Flexible Nanoelectronics. *Adv. Mater.* **2023**, *35*, 2301280.

(24) Jiang, F.; Poh, W. C.; Chen, J.; Gao, D.; Jiang, F.; Guo, X.; Chen, J.; Lee, P. S. Ion Rectification Based on Gel Polymer Electrolyte Ionic Diode. *Nat Commun* **2022**, *13*, 6669.

(25) Tybrandt, K.; Gabrielsson, E. O.; Berggren, M. Toward Complementary Ionic Circuits: The *Npn* Ion Bipolar Junction Transistor. *J. Am. Chem. Soc.* **2011**, *133*, 10141–10145.

(26) Ye, Y.; Yu, L.; Lizundia, E.; Zhu, Y.; Chen, C.; Jiang, F. Cellulose-Based Ionic Conductor: An Emerging Material toward Sustainable Devices. *Chem. Rev.* **2023**, *123*, 9204–9264.

(27) Zhang, W.; Zhang, X.; Lu, C.; Wang, Y.; Deng, Y. Flexible and Transparent Paper-Based Ionic Diode Fabricated from Oppositely Charged Microfibrillated Cellulose. *J. Phys. Chem. C* **2012**, *116*, 9227–9234.

(28) Nyamayaro, K.; Keyvani, P.; D'Acierno, F.; Poisson, J.; Hudson, Z. M.; Michal, C. A.; Madden, J. D. W.; Hatzikiriakos, S. G.; Mehrkhodavandi, P. Toward Biodegradable Electronics: Ionic Diodes Based on a Cellulose Nanocrystal–Agarose Hydrogel. *ACS Appl. Mater. Interfaces* **2020**, *12*, 52182–52191.

(29) Klemm, D.; Kramer, F.; Moritz, S.; Lindström, T.; Ankerfors, M.; Gray, D.; Dorris, A. Nanocelluloses: A New Family of Nature-Based Materials. *Angew. Chem. Int. Ed.* **2011**, *50*, 5438–5466.

(30) De France, K.; Zeng, Z.; Wu, T.; Nyström, G. Functional Materials from Nanocellulose: Utilizing Structure–Property Relationships in Bottom-Up Fabrication. *Adv. Mater.* **2021**, *33*, 2000657.

(31) Abdul Khalil, H. P. S.; Davoudpour, Y.; Islam, Md. N.; Mustapha, A.; Sudesh, K.; Dungani, R.; Jawaid, M. Production and Modification of Nanofibrillated Cellulose Using Various Mechanical Processes: A Review. *Carbohydrate Polymers* **2014**, *99*, 649–665.

(32) Rol, F.; Belgacem, M. N.; Gandini, A.; Bras, J. Recent Advances in Surface-Modified Cellulose Nanofibrils. *Progress in Polymer Science* **2019**, *88*, 241–264.

(33) Yang, W.; Lv, L.; Li, X.; Han, X.; Li, M.; Li, C. Quaternized Silk Nanofibrils for Electricity Generation from Moisture and Ion Rectification. *ACS Nano* **2020**, *14*, 10600–10607.

(34) Quellmalz, A.; Mihranyan, A. Citric Acid Cross-Linked Nanocellulose-Based Paper for Size-Exclusion Nanofiltration. *ACS Biomater. Sci. Eng.* **2015**, *1*, 271–276.

(35) Yang, H.; Edberg, J.; Gueskine, V.; Vagin, M.; Say, M. G.; Erlandsson, J.; Wågberg, L.; Engquist, I.; Berggren, M. The Effect of Crosslinking on Ion Transport in Nanocellulose-Based Membranes. *Carbohydrate Polymers* **2022**, *278*, 118938.

(36) Kono, H.; Ogasawara, K.; Kusumoto, R.; Oshima, K.; Hashimoto, H.; Shimizu, Y. Cationic Cellulose Hydrogels Cross-Linked by Poly(Ethylene Glycol): Preparation, Molecular Dynamics, and Adsorption of Anionic Dyes. *Carbohydrate Polymers* **2016**, *152*, 170–180.

(37) Pei, A.; Butchosa, N.; Berglund, L. A.; Zhou, Q. Surface Quaternized Cellulose Nanofibrils with High Water Absorbency and Adsorption Capacity for Anionic Dyes. *Soft Matter* **2013**, *9* (6), 2047.

(38) Yamamoto, T.; Doi, M. Electrochemical Mechanism of Ion Current Rectification of Polyelectrolyte Gel Diodes. *Nat Commun* **2014**, *5*, 4162.

(39) Macher, S.; Rumpel, M.; Schott, M.; Posset, U.; Giffin, G. A.; Löbmann, P. Avoiding Voltage-Induced Degradation in PET-ITO-Based Flexible Electrochromic Devices. *ACS Appl. Mater. Interfaces* **2020**, *12*, 36695–36705.

Supporting Information

Study on the Rectification of Ionic Diode Based on Cross-linked Nanocellulose Bipolar Membranes

Hongli Yang,[a,b,*] *Jesper Edberg,*[c] *Mehmet Girayhan Say,*[b] *Johan Erlandsson,*[d] *Viktor Gueskine,*[b,e] *Lars Wågberg,*[d,f] *Magnus Berggren,*[b,e] *Isak Engquist*[b,e]

[a]College of Polymer Science and Engineering, Sichuan University, Chengdu 610065, P. R. China.

[b]Laboratory of Organic Electronics, Department of Science and Technology, Linköping University, SE-601 74 Norrköping, Sweden

[c]RISE Research Institutes of Sweden, Digital Systems, Smart Hardware, Bio-, Organic and Printed Electronics, Norrköping 60233, Sweden.

[d]Division of Fibre Technology, Department of Fibre and Polymer Technology, School of Chemistry, Biotechnology and Health, KTH Royal Institute of Technology, SE-100 44 Stockholm, Sweden.

[e]Wallenberg Wood Science Centre, Department of Science and Technology, Linköping University, SE-601 74 Norrköping, Sweden.

[f]Wallenberg Wood Science Centre, Department of Fibre and Polymer Technology, School of Chemistry, Biotechnology and Health, KTH Royal Institute of Technology, SE-100 44 Stockholm, Sweden.

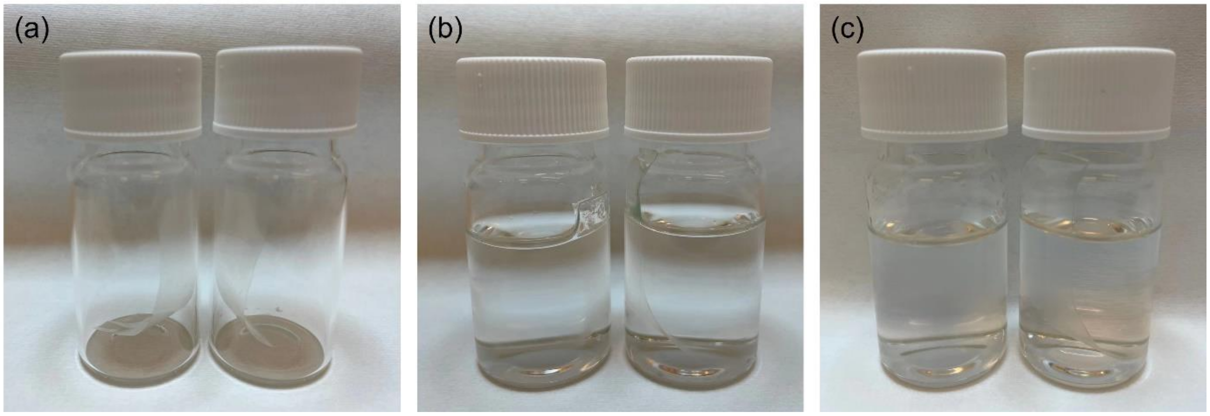

Figure S1. Real pictures of non-crosslinked (left) and PEGDE crosslinked (right) cationic CNF membranes in different conditions: (a) membranes in a dry state; (b) membranes were immersed in water for 1 min; (c) membranes were immersed in water for one week.

In Figure S1, the real pictures of non-crosslinked and PEGDE crosslinked cationic CNF membranes before and after the immersion in water are shown. When they are dry, both non-crosslinked and crosslinked membranes are flexible (Figure S1a). After being immersed in water, the non-crosslinked membrane swells quickly, and the fibrils gradually disperse in the water to form a dispersion, like the gel after one week. Meanwhile, the crosslinked CNF membrane keeps stable even if it is immersed in water for one week. It indicates that the crosslinking of cationic CNF is indeed successful by using PEGDE as a crosslinker. On the other hand, crosslinking can significantly enhance the water stability of the cationic CNF membrane.

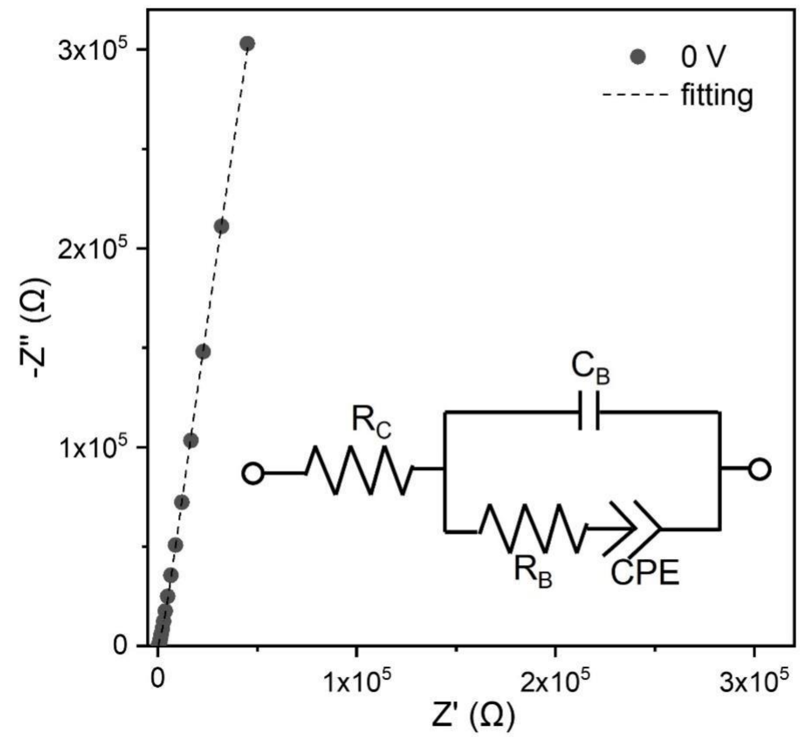

Figure S2. Nyquist plot of AC-impedance measurement of 50 μm ACNF + 55 μm CCNF bipolar membrane, dash line represents the fit of the equivalent circuit model shown in the inset.

The equivalent circuit model to fit the Nyquist plot is referred to as the one for ionoelastomer junction.[1] It contains a resistor corresponding to contact resistance; a dielectric capacitance (C_B) corresponding to the polarization of the ionic diode at high frequency; another resistor (R_B) which is connected in parallel with C_B indicates the ion transport at moderate frequency; a constant phase element (CPE) describes the formation of an ionic double layer at the interface at low frequency.

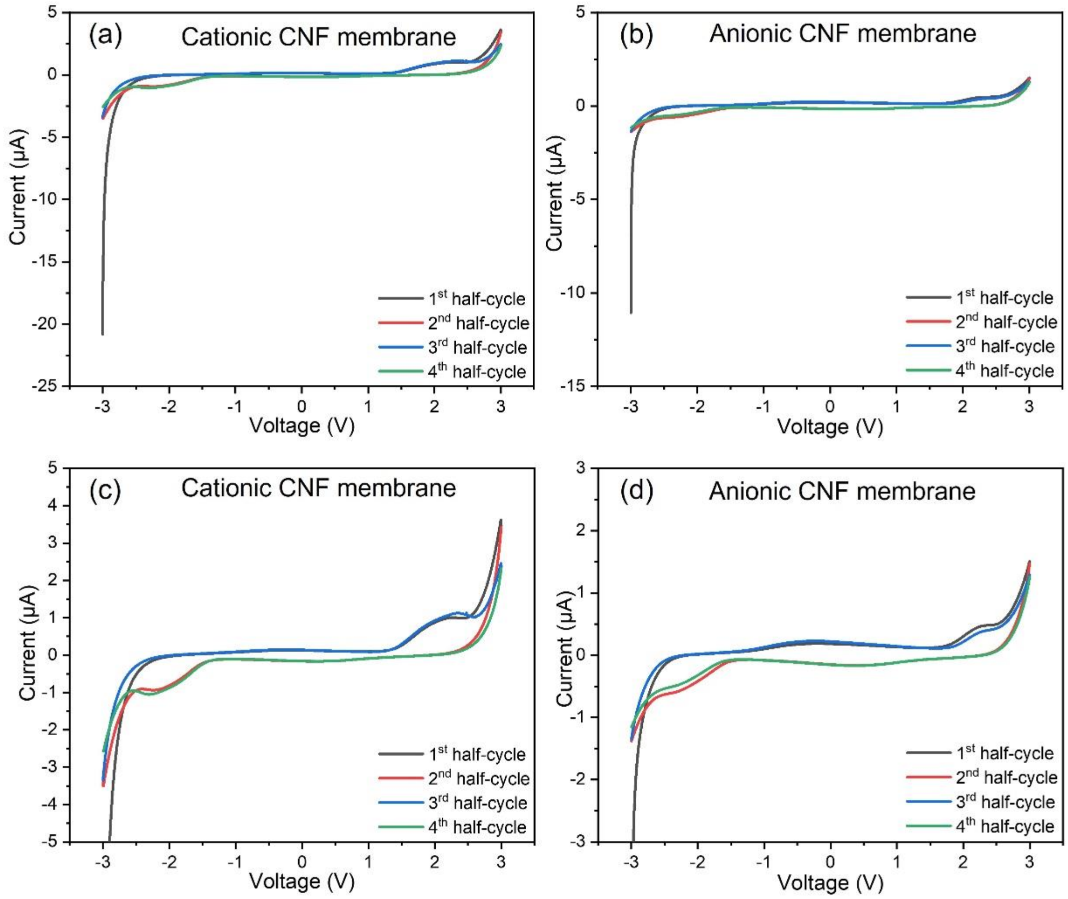

Figure S3. Current as a function of applied bias plots with two sweeping cycles for (a) PEGDE crosslinked cationic CNF monolayer membrane and (b) BTCA crosslinked anionic CNF monolayer membrane with the scan rate of 5 mV/s under the voltage range from -3 V to 3 V. (c) enlarged view of (a); (d) enlarged view of (b).

The current-voltage characteristics of crosslinked cationic or anionic monolayer membranes measured by the linear sweeping of applied voltages are shown in Figure S3. Same with the bipolar membrane, there is a current that drops quickly at the beginning of sweeping for both cationic and anionic single membrane, which is caused by the transport of counterions inside the membrane due to the suddenly applied voltage. After the first sweeping half-cycle, there is no clear rectifying behavior for both cationic and anionic single membranes. In addition, the maximum currents under forward and backward biases slightly decrease with the sweeping cycle, resulting from the consumption of water during the measurement.

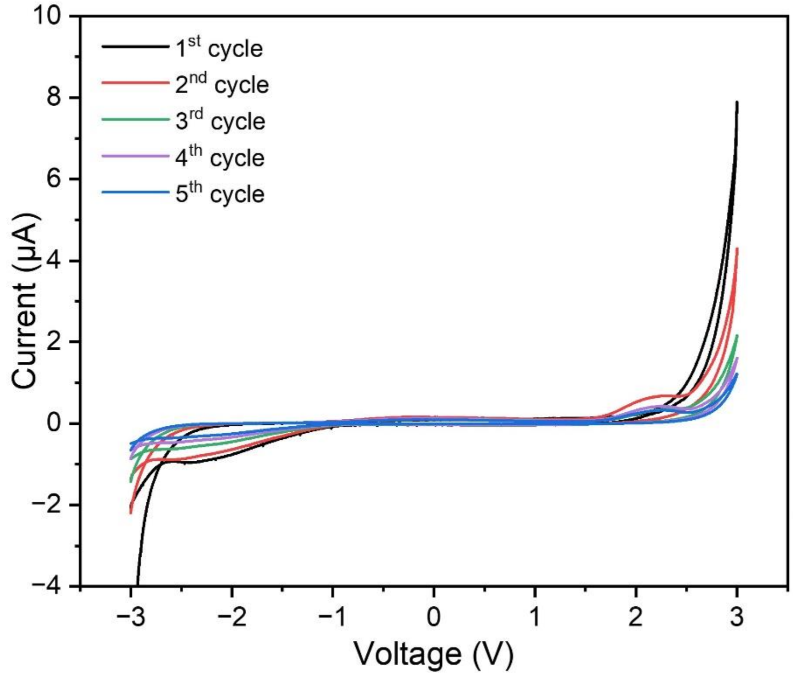

Figure S4. Current as a function of applied bias plots with 5 sweeping cycles for 50 μm ACNF + 55 μm CCNF bipolar membrane with the scan rate of 5 mV/s under the voltage range of -3 V − +3 V.

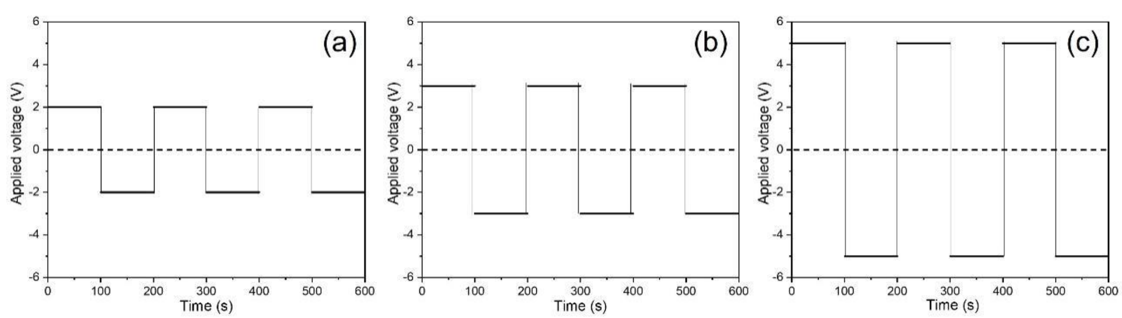

Figure S5. The applied voltage with time plot corresponds to Figure 7 (a)-(c) in the main manuscript.

REFERENCES

(1) Kim, H. J.; Chen, B.; Suo, Z.; Hayward, R. C. Ionoelastomer Junctions between Polymer Networks of Fixed Anions and Cations. *Science* **2020**, *367*, 773–776.